# SEMICONDUCTOR WAVEGUIDE GRATINGS

By

**Ramesh Kumar Sonkar**



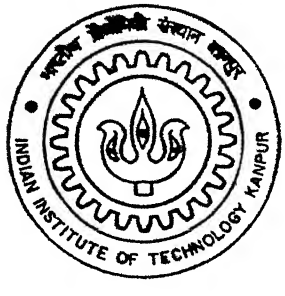


DEPARTMENT OF ELECTRICAL ENGINEERING

**Indian Institute of Technology Kanpur**

MAY, 2003

# SEMICONDUCTOR WAVEGUIDE GRATINGS

*A Thesis Submitted*

*In Partial Fulfillment of the requirements*

*For the Degree of*

MASTER OF TECHNOLOGY

by

Ramesh Kumar Sonkar

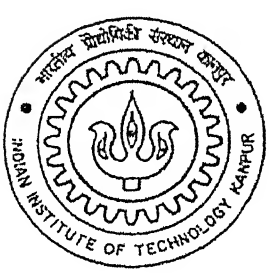


to the

**DEPARTMENT OF ELECTRICAL ENGINEERING**

**INDIAN INSTITUTE OF TECHNOLOGY KANPUR**

**May 2003**

# CERTIFICATE

It is certified that the work contained in this thesis titled **"SEMICONDUCTOR WAVEGUIDE GRATINGS"**, by RAMESH KUMAR SONKAR, has been carried out under my supervision and this work has not been submitted elsewhere for a degree.

Dr. Utpal Das
Professor
Department of Electrical Engineering
Indian Institute of Technology Kanpur

May 2003

# ACKNOWLEDGEMENT

It is my privilege to express my sincere gratitude to my thesis supervisor Dr. Utpal Das, for his excellent and skilled guidance. I am deeply indebted to my supervisor Dr.Utpal Das whose help, stimulating suggestions and encouragement helped me in all the time of research for and writing of this thesis. His broad and profound knowledge, his warm smile and his patient instruction have given me a great help, I owe him lots of gratitude for having me shown this way of research. He could not even realize how much I have learned from him.

I am grateful to all my colleagues and friends who gave me the feeling of being at home at work T.Venkatesh, Neeraj Sharma, Manoj Panda, Pankaj Kumar, A.Shivabalan, B.Rami Reddy and Ankush Jain need a special mention for all their help and support.

I can never adequately thank to my father, all my brothers and all my family members who encouraged me to study and gave me all support and their LOVE for me all the times. I could reach here only because of my Parents.

I.I.T. Kanpur Ramesh Kumar Sonkar

To

# My Parents and Gurus

# ABSTRACT

Distributed Bragg gratings have been analyzed for the purpose of its usage as reflectors for the discrimination of wavelengths pertaining to optical communications. Coupled mode theory and simple Bragg reflection methods have been used to calculate the reflection coefficient of periodically perturbed dielectric optical waveguides. The analysis has been done for both first order and second order gratings. First order grating show larger discrimination however their physical dimensions are difficult to realize by simple photolithography. Second order grating show that they are realizable for 1270nm-1610nm-wavelength range for periodic dimensions of 0.5-1.2μm. A practical case of periodic change in the refractive index by Impurity Implantation Disordering of quantum wells have also been considered. The analytical expressions for the coupling and reflection coefficients are given for the case of an asymmetric trapezoidal grating profile with a view to having different thicknesses of the multiquantum well layer. The lateral spread of the implanted impurity was modeled by a trapezoidal profile.

The observation from the simulation plots of groove height with reflection coefficient shows, as we increase frequency from 1270nm –1610nm the groove height shifts towards right. The plots of distance with reflection coefficient also shows, increase in the frequency results right shift in the distance.

# CONTENTS


| | | | |
|---|---|---|---|
| Title | | | i |
| Certificate | | | ii |
| Acknowledgement | | | iii |
| Abstracts | | | v |
| Contents | | | vi |
| List of figures | | | vii |
| **Chapter 1:** | | **Introduction** | 1 |
| **Chapter** | **2:** | **Simulation** | 7 |
| | 2.1 | Grating Characterizations | 7 |
| | 2.2 | Coupled Mode Theory | 9 |
| | 2.3 | Coupled Mode Equations | 13 |
| | 2.4 | Contradirectional Coupling | 14 |
| | 2.5 | Bragg Reflection | 16 |
| | 2.6 | Analysis of trapezoidal grating | 18 |
| **Chapter** | **3:** | **Results and Discussion** | 21 |
| | 3.1 | Reflection Coefficient of Bragg Gratings | 21 |
| | 3.2 | Reflectivity of the Trapezoidal grating | 26 |
| **Chapter** | **4:** | **Conclusions** | 32 |
| | | **References** | 34 |

# LIST OF FIGURES


| | | |
|---|---|---|
| Figure.1.1. | Schematic of a grating-assisted coupler with grating located on the lower slab | 5 |
| Figure.2.1. | Corrugated slab waveguide | 7 |
| Figure.2.2. | Gratings viewed from above:(a) Tilt and (b) Curved | 8 |
| Figure.2.3. | Two-dimensional corrugated waveguide:(a) in perspective And (b) cross section | 10 |
| Figure 2.4. | Top: a corrugated section of a dielectric waveguide. Bottom: the incident and reflected intensities inside the corrugated section | 15 |
| Figure.2.5. | A schematic drawing of a periodic layered medium and the plane-wave amplitudes associated with the *n*th unit cell and its neighboring layers | 17 |
| Figure.3.1. | Distance ($d_1$) dependence on Reflection Coefficients at various Wavelength with N=100 | 22 |
| Figure.3.2. | Distance ($d_1$) dependence on Reflection Coefficients at various Wavelength with N=200 | 23 |
| Figure.3.3. | Wavelength ($\lambda$) dependence on Reflection Coefficients at various N with Distance ($d_1$=0.615μm) | 24 |
| Figure.3.4. | Wavelength ($\lambda$) dependence on Reflection Coefficients at various N with Distance ($d_1$=0.615μm) | 25 |
| Figure.3.5. | (a) Reflection Coefficient as a function of Distance $d_1$ at various wavelength with groove height 'g' of 480 nm, m=2 and angle is 20° (b) Coupling Coefficient as a function of Normalised Distance ($L_2/\Lambda_z$) at various wavelength with groove height 'g' of 480 nm, m=2 and angle is 20°. | 27 |
| Figure.3.6. | (a) Reflection Coefficient as a function of Tooth Height (g) [μm] at various wavelength with Distance '$d_1$' of 600nm, m=2 and angle is 20° (b) Coupling Coefficient as a function of Tooth Height (g) [μm] at various wavelength with Distance '$d_1$' of 600nm, m=2 and angle is 20°. | 28 |
| Figure.3.7. | (a) Reflection Coefficient as a function of Mode Number at various wavelength with distance of 600 nm, groove height of 400nm and angle is $20^0$ (b) Coupling Coefficient as a function Mode Number at various wavelength with distance of 600 nm and angle is 20 degree | 29 |
| Figure.3.8. | (a) Variation of Reflection Coefficient with Wavelength at various Distance $d_1$ [nm] with groove height of 480nm, angle is $20^0$ and m=2. (b) Variation of Coupling Coefficient with Wavelength at various Distance $d_1$ [nm] with groove height of 480nm, angle is $20^0$ and m=2. | 30 |
| Figure 3.9. | Comparison of the second mode reflection coefficients of the grating at Wavelength Separations of 20nm as required for Coarse Wavelength Division Multiplexing at g=200nm | 31 |

# Chapter 1

# INTRODUCTION

Semiconductor optoelectronic devices have currently become popular in various everyday applications such as optical fiber communications, laser printers, compact discs, sensors etc. The need for improving the performances of these optoelectronic systems have led to the emergence of optoelectronic integration technology, where different optoelectronic components are integrated on the same chip. The periodic corrugated waveguide structures have been employed for a variety of purposes. Bragg grating's are now used for mode selectivity resulting in the suppression of unwanted modes of lasers, which otherwise limits the optical information rate. Small periodic perturbations in a guided wave device can also facilitate the interaction of various optical waves. Grating structures thus have wide applicability in optical devices such as distributed reflector for distributed feedback (DFB) lasers [1], distributed Bragg reflector (DBR) lasers [2], wavelength filters [3], input and output couplers, multiplexers [4], dispersion compensators, resonators and some non linear processes. To date the analysis of these structures has taken into account the waveguide perturbation in one transverse direction and of course their periodic variation along the propagation direction. In actuality, however, waves are limited in both transverse directions either by a two-dimensional waveguide or as a result of the finite lateral extent of the wave itself. The finite lateral wave width is particularly important in the grating analysis if the grating teeth are slightly misaligned with respect to the propagation direction or if the grating is curved. The former situation arises either inadvertently, or when one wishes to change the resonant wavelength or radiation direction by varying the effective grating period by introducing tilt. The latter case has other possible applications. More recently, corrugations have been used in high power

DBR surface emitting diode lasers and laser arrays and several laboratories are involved in the fabrication of such devices [5-7].

In these applications both distributed Bragg reflectors (DBR) and distributed feedback (DFB) configurations were employed to select and stabilize wavelength. Distributed feedback (DFB) lasers differ from conventional lasers in that feedback is provided by a distributed periodic spatial variation in gain, refractive index, and/or geometry, rather than by discrete reflectors. The analysis of these devices [7] has been carried out as a function of the coupling coefficient $\kappa$, which describes the degree to which reverse propagating waves transfer energy. Generally, $\kappa$ has been expressed in terms of refractive index and/or gain variations, which perturb the light. The motivation for incorporating a quantum well active layer in a DFB laser includes a tenfold thinning of the active region over that of a conventional semiconductor laser region, which results in significant threshold current reductions. Other advantages include narrower line width, higher speed response and higher output power. It is well known that InP, InGaAs, etc. based semiconductors and multi-quantum well (MQW) structures exhibit large optical non-linearities resulting from intensity dependent absorption and refractive index changes at wavelengths near the band edge. Therefore, an intensity dependent MQW refractive index nonlinearity must be considered, especially for high power lasers. Optical nonlinearities may result in a change from the linear case of the ratio of the rating power to the total transverse mode. Distributed-feedback (DFB) lasers are of fundamental interest in long distance communications. High-speed semiconductor DFB and DBR lasers are crucial for high-speed optical communication links. These lasers can be directly modulated at frequencies reaching 20 to 30 GHz. They have important applications in optical links based upon WDM (Wavelength Division Multiplexing) technology. Direct laser modulation schemes are much simpler

to implement and integrate than modulation schemes based upon external modulators. However, modulation bandwidth of external modulators can easily go beyond 60 GHz. Thus, it is technologically important to have DFB/DBR lasers whose modulation bandwidths compete with those of external modulators. High performance DFB and DBR lasers demand that careful attention be paid to the design of the grating, which provides the optical feedback. Spatial hole burning, side mode suppression, radiation loss, laser line width, spontaneous emission in non-lasing modes, lasing wavelength selection and tunability, laser relaxation oscillation frequency etc. are all features that are very sensitive to the grating design. Improved grating design can significantly enhance laser performance, especially at higher modulation frequencies.

Grating coupled distributed Bragg reflector (DBR) lasers have great flexibility in the fabrication of surface emitting lasers. They are particularly attractive when single mode operation is required. Conventional grating coupled surface emitting lasers have difficulties in providing a beam with circular cross section. Quantum wells and strained quantum wells are widely used as active structures. This is because Quantum wells offers unique properties such as carrier confinement, step like density of states, tunneling, quantum confined stark effect, high electron mobility, nonlinearity etc.

Optical communications by dense wavelength division multiplexing (DWDM or WDM), which uses a number of wavelengths and a signal on each wavelength channel for transmission, has made massive progress as high-speed, high-capacity optical communication system for the Internet age. A crucial device in this kind of communication system is the optical wavelength filter used to separate out the wavelengths. The filtering properties of periodic structures are well known and have been exploited in various optical devices where the periodic perturbation is often induced by means of grating. A popular technique for studying such structures in the

coupled mode theory [6] despite the development of the alternative mode matching technique [8]. These, although more precise, are only practical for rectangular gratings. In contrast, the coupled mode technique is straightforward and applicable to any kind of grating shape and provides good results when the refractive index perturbation is small as in most integrated optic devices. DWDM systems are relatively expensive and medium to short-haul networks, are very cost sensitive although network traffic is quite large. There is a new trend to use the so-called coarse wavelength division multiplexing (CWDM) systems in these networks to lower the cost dramatically while still provide sufficient bandwidth capacity. Dense Wavelength Division Multiplexing (DWDM) can put up to 40 wavelengths in what is called the C band, from 1530 nm to 1565 nm, or 1 wavelength every 0.8 nm. Coarse Wavelength Division Multiplexing (CWDM) technology spaces 18 channel signals at 20 nm meter intervals and spaces 1270-1630nm without much concern of losses in the new zero loss fiber at 1100nm.

There has been increasing interest in grating-assisted optical directional couplers lately due to their potential applications in the integrated photonic systems based on wavelength division multiplexing. The coupled mode theory is often adopted for the analysis of the grating assisted couplers. The primary structures of interest are grating-assisted couplers in which two or more co propagating modes interact through a longitudinal surface or index corrugation. A schematic diagram of the grating-assisted coupler is depicted in Figure1.1. The grating serves the purpose of matching the propagation constants of the guided modes to achieve synchronous power transfer between them. In addition the grating simultaneously matches the guided modes to a narrow bandwidth of the spectrum. Grating-assisted directional couplers are widely used in the design of optical waveguide filters [9]. A basic configuration of the couplers

consists of nonidentical waveguides placed adjacently in which a periodic grating structure is embedded coupling region.

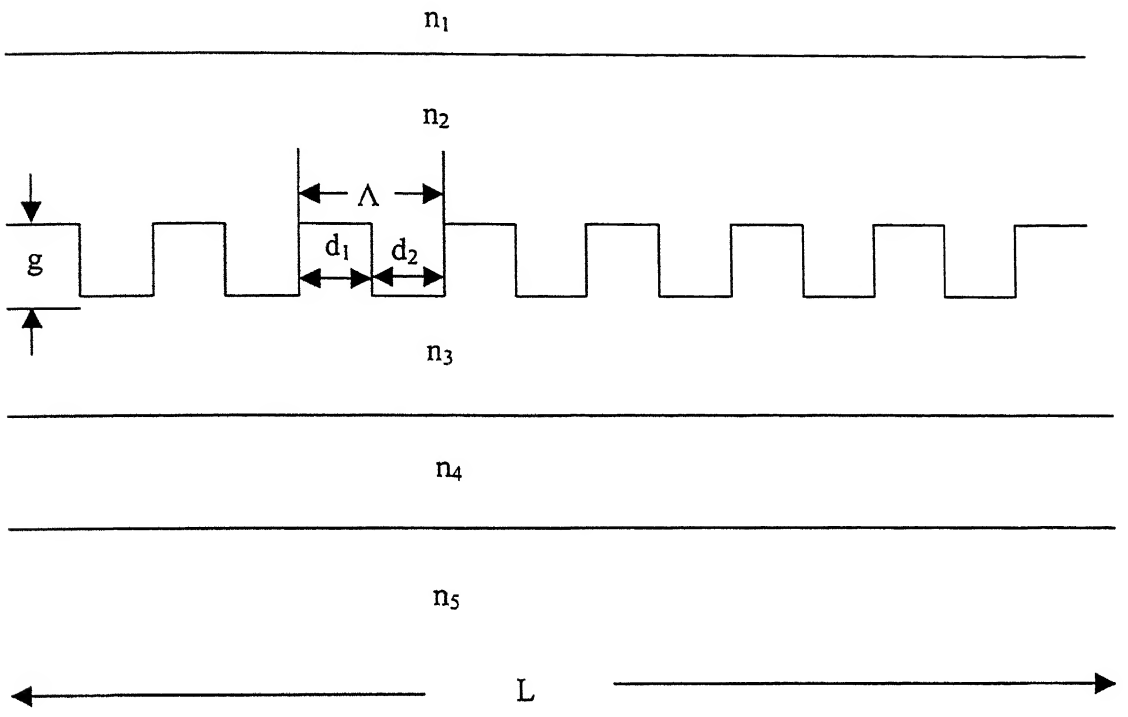


Figure.1.1.Schematic of a grating-assisted coupler with grating located on the lower slab

The phase synchronism in two nonsynchronous waveguides is achieved through the space-harmonic components generated by the grating. When the grating period is specified, a complete power transfer from one guide to the other is obtained at a particular wavelength satisfying the phase-matching condition. This makes the coupler wavelength selective. $\Lambda=d_1+d_2$ constitutes the period of the grating and the typical dimensions of $d_1$or $d_2$ ~ 200nm. This is however difficult to fabricate using normal integrate circuit technology. This is specially true when several gratings with several different periods are needed on the same area of the chip. Instead of the current technique of etch and regrowth one may use a MQW region whose energy/refractive index maybe periodically altered by impurity implantation and anneal (IILD).

Therefore $d_1$ or $d_2$ will be width of the mask through which implantation needs to be performed.

$d_1$ and $d_2$ cannot have dimensions of the order of 200nm because of the lateral diffusion of the dopants. So for this case one needs to find a situation where $d_1$ and $d_2$ are larger and separation between wavelengths are also large so that we have a broadband spectrum around 1.55μm. In the present work it is intended that the grating provides adequate at the interval of 20nm for the CWDM for a second order grating with $d_1$ and $d_2$ of the order of 0.5 μm to 0.8 μm. The reflection coefficient with the variation of groove height, wavelength, order, $d_1$ and $d_2$ and groove angle have been calculated. These results have been used to investigate the performance of optoelectronic devices. In the second chapter, description of the coupled mode theory to calculate coupling coefficient and reflection coefficient is given. It begins with a theoretical description of coupled mode equations and analytical description of the misaligned or curved gratings are given. The third chapter describes the results obtained from a simulation of the theory presented in the previous sections with detailed discussion. The final chapter concludes the work with projection of this work for future study.

# Chapter 2

# SIMULATIONS

## 2.1 Grating Characterizations

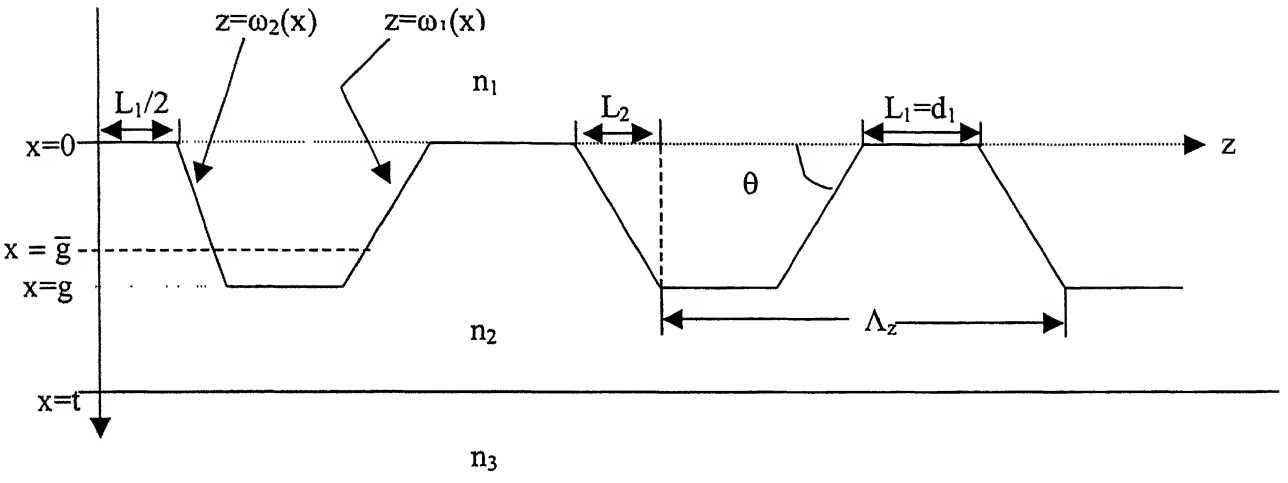


Figure.2.1. Corrugated slab waveguide.

A typical corrugated slab waveguide is shown in Figure 2.1. The functions $w_1(x)$ and $w_2(x)$ describe the tooth shape, $\Lambda_z$, is the period, g is the tooth height, and the refractive indices are $n_1$ , $n_2$ , and $n_3$. In the grating region, $0 < x < g$, the refractive index variation is [10]

$$N^2(x, z)= \sum_{p=-\infty}^{\infty} (n_1^2\{u [z-w_1 (x)+p\Lambda_z]-u[z-w_2(x)+ p\Lambda_z]\}$$

$$+n_2^2\{u [z-w_2 (x)+p\Lambda_z]-u[z-w_1(x)+ (p-1)\Lambda_z]\}) \quad (1)$$

where

$$u(\varsigma)=\begin{cases}1, & \varsigma > 0\\ 0, & \varsigma < 0\end{cases} \quad (2)$$

the Fourier expansion of the periodic function (1) is in the form

$$n^2(x,z)= \sum_{q=-\infty}^{\infty} A_q(x)\exp(i2\pi qz/\Lambda_z) \quad (3)$$

and

$$A_q(x) = \begin{cases} n_2^2 - \left(n_2^2 - n_1^2\right)\left[w_2(x) - w_1(x)\right]/\Lambda_z, & q = 0 \\ \dfrac{\left(n_2^2 - n_1^2\right)}{i2q\pi}\left\{\exp\left[-i2\pi q w_2(x)/\Lambda_z\right] - \exp\left[-i2\pi q w_1(x)/\Lambda_z\right]\right\}, & q \neq 0 \end{cases} \quad \text{(4a \& 4b)}$$

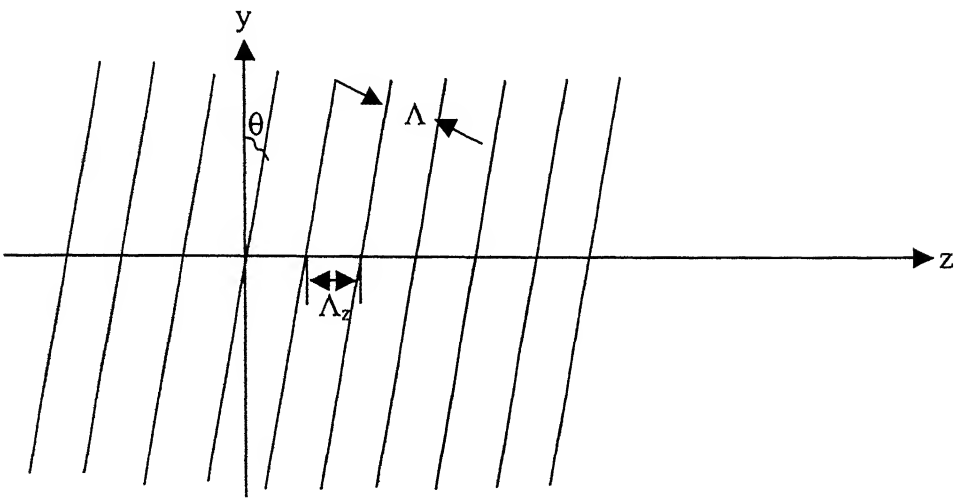


(a)

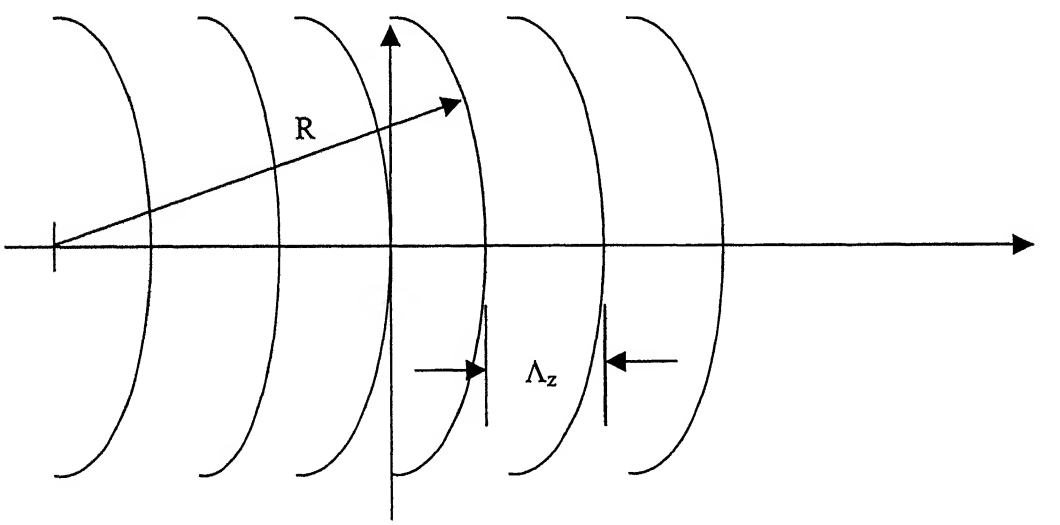


(b)

Figure.2.2.Gratings viewed from above:(a) Tilt and (b) Curved.

Fortunately, the above representation applies as well to tilted or curved gratings, such as are illustrated in Figure. 2.2(a) and 2.2(b). For a grating tilted at $\theta$,

$$\Lambda_z = \Lambda/\cos\theta \tag{5}$$

and

$$n_t^2(x,y,z) = n^2(x,0,z - y\tan\theta),\ 0<x<g, \tag{6}$$

whereas for the grating of radius R,

$$n_c^2(x,y,z) = n^2(x,0,z+R-\sqrt{(R^2-y^2)}),\ 0<x<g. \tag{7}$$

Upon combining (6) or (7) with (3), one obtains

$$n^2(x,y,z) = A_q(x)N_q(y)\exp i2\pi qz/\Lambda_z,\quad 0<x<g \tag{8}$$

where

$$N_q(y) = \begin{cases} \exp(-(i2\pi qy\tan\theta)/\Lambda_z), & \textit{tilt} \\ \exp\left(i\pi\pi\left(R-\sqrt{(R^2-y^2)}\right)/\Lambda_z\right) & \textit{curvature} \end{cases} \tag{9a\&9b}$$

Clearly, more complicated variations (e.g., tilt plus curvature) may be similarly represented.

Obviously, for $\theta = 0$ or $R = \infty$, (9a) and (9b) reduce to the one-dimensional result $N_q \equiv 1$. Moreover, we observe that for $q \neq 0$ the terms are in a particularly convenient form containing products of the three spatial variables. The term $A_o(x)$ is unaffected by tilt or curvature. As previously noted [9], it equals the average of $n^2(x, z)$ taken along z for every x.

## 2.2 Coupled Mode Theory

Consider the two-dimensional corrugated waveguide shown in perspective as Figure. 2.3(a) and in cross section as Figure. 2.3(b). Such structures support modes with $E_x \approx 0$, which are analogous to TE modes in the slab waveguide. Their $E_y$ field component satisfies

$$[\frac{\partial^2}{\partial x^2}+\frac{\partial^2}{\partial y^2}+\frac{\partial^2}{\partial z^2}+k_o^2n^2(x,y,z)]E_y(x,y,z)=0, \tag{10}$$

$$\Lambda_z=\Lambda/\cos\theta.$$

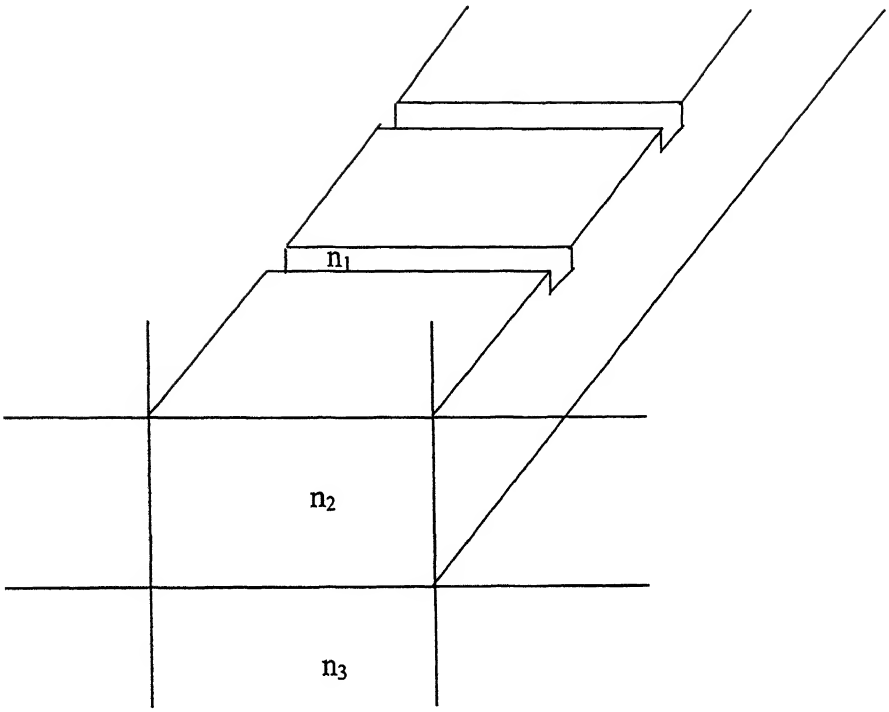


(a)

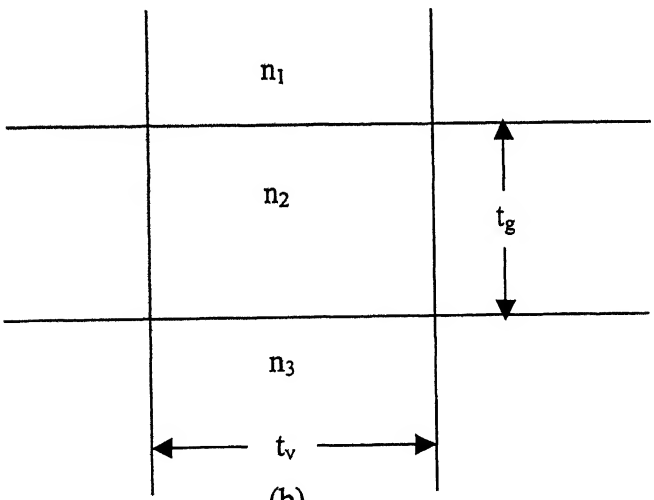


(b)

Figure.2.3. Two-dimensional corrugated waveguide:
(a) in perspective and (b) cross section

where $k_o = 2\pi/\lambda_o$ and $\lambda_o$ is the free space wavelength. For the case of coupled contradirectional modes a solution in the form

$$E_{,}(x,y,z) = \tilde{R}(z)E_{r}(x,y)\exp(i\beta_{r}z) + S(z)E_{s}(x,y)\exp(-i\beta_{s}z), \quad (11)$$

where $E_r$ (x, y) is the mode propagating in the z-direction and $\tilde{R}(z)$ is a slowly varying complex function. The mode pattern $E_s$ (x, y) and function S (z) fulfill the same roles for the mode propagating in the opposite direction. For hybrid or inter-mode coupling, $E_r$ (x, y) and $E_s$ (x, y) differ in their x - and/or y-variations, whereas $E_r \equiv E_s$ in the intramode situation. If contradirectional coupling is to occur, there must exist some free space wavelength $\lambda_a$ for which

$$\beta_r + \beta_s = \frac{2\pi m}{\Lambda_z} \quad , \quad (12)$$

where m is an integer and $\beta_r$ , $\beta_s$ are calculated at $\lambda_a$ for the waveguide without a corrugation. Clearly, since $\Lambda_z$ appears in (12) in place for $\Lambda$ for an aligned grating, the wavelength dependent effects of tilt are described by the cos $\theta$ variation in (5), viz

Next, the complete refractive index spatial variation is rewritten

$$n^2(x,y,z) = n_0^2(x,y) \sum_{\substack{q=-\infty \\ q\neq 0}}^{\infty} A_q(x)N_q(y)\exp(i2\pi qz/\Lambda_z), \quad (13)$$

where $n_0^2$(x, y) contains the full two-dimensional variation of Fig. 4(b) together with $A_0$(x) in the grating region, and the summation terms are zero outside the grating. Since the unperturbed dielectric medium is homogeneous in the z direction [i.e., $\partial\varepsilon_0(x,y)/\partial z = 0$ ], the normal modes can be written in the form

$$E_m(x,y)e^{i(\omega t - \beta_m z)}, \quad (14)$$

where the m is the mode subscript, which can be either continuous for unbound modes, such as plane waves ,or discrete for confined modes, such as waveguide modes[11]. These normal modes satisfy

$$\left[\frac{\partial^2}{\partial x^2} + \frac{\partial^2}{\partial y^2} + \omega^2\mu\varepsilon_0(x,y) - \beta_m^2\right]E_m(x,y) = 0 \quad (15)$$

If an arbitrary field of frequency ω is excited, the propagation of this field in the normal modes of the unperturbed dielectric structure, where the expansion coefficients evidently depend on $z$, since for $\Delta\varepsilon \neq 0$ the waves $E_m(x,y)e^{i(\omega t-\beta_m z)}$ are no longer eigenmodes:

$$E = \sum_m A_m(z)E_m(x,y)e^{i(\omega t-\beta_m z)} \tag{16}$$

where $A_m$` are constants. Substituting Eq. (16) into the wave equation Eq.(15)

$$\{\nabla^2 + \omega^2\mu[\varepsilon_0(x,y)+\Delta\varepsilon(x,y,z)]\}E = 0 \tag{17}$$

and using Eq.(15),

$$\sum_k\left[\frac{d^2}{dz^2}A_k - 2i\beta_k\frac{d}{dz}A_k\right]E_k(x,y)e^{-i\beta_k z} = -\omega^2\mu\sum_l \Delta\varepsilon(x,y,z)A_l E_l(x,y)e^{-i\beta_l z} \tag{18}$$

we now assume further that dielectric perturbation is "weak," so that the variation of the mode amplitudes is "slow" and satisfies the condition

$$\left|\frac{d^2}{dz^2}A_k\right| << \left|\beta_k\frac{d}{dz}A_k\right| \tag{19}$$

This condition is known as parabolic approximation and is often used when the perturbation is small. Thus, neglecting the second derivative in Eqs. (18) leads to

$$-2i\sum_k\beta_k\left(\frac{d}{dz}A_k\right)E_k(x,y)e^{-i\beta_k z} = -\omega^2\mu\sum_l \Delta\varepsilon(x,y,z)A_l E_l(x,y)e^{-i\beta_l z} \tag{20}$$

Since the dielectric perturbation $\Delta\varepsilon$ (x, y, z) is periodic in z, we can expand it as a Fourier series

$$\Delta\varepsilon(x,y,z) = \sum_{m\neq 0}\varepsilon_m(x,y)\exp\left[-im\frac{2\pi}{\Lambda}z\right] \tag{21}$$

where the summation over all m except m=0 because of the definition of $\Delta\varepsilon(x,y,z)$ in

$$\varepsilon(x,y,z) = \varepsilon_0(x,y) + \Delta\varepsilon(x,y,z) \tag{22}$$

Substitution of Eq. (21) in Eq. (20) leads to

$$\frac{d}{dz}A_k = -i\frac{\beta_k}{|\beta_k|}\sum_l\sum_m C_{kl}^{(m)}A_l e^{i(\beta_k-\beta_l-m2\pi/\Lambda)} \tag{23}$$

where the coupling coefficient $C_{kl}^{(m)}$ is defined as

$$C_{kl}^{(m)} \equiv \frac{\omega}{4}\langle k\ \varepsilon_m\ l\rangle = \frac{\omega}{4}\int E_k^*(x,y)\varepsilon_m(x,y)E_l(x,y)\,dx\,dy \tag{24}$$

This coefficient $C_{kl}^{(m)}$ reflects the magnitude of coupling between k*th* and l*th* modes due to the m*th* Fourier component of the dielectric perturbation.

Equation (23) constitutes a set of coupled linear differential equation. In principle, an infinite number of mode amplitude are involved. However in practice only two modes are strongly coupled and Eq. (23) reduces to two equations for the two mode amplitudes. By resonant coupling, we mean a mode coupling at the condition when

$$\beta_k - \beta_l - m\frac{2\pi}{\Lambda} = 0 \tag{25}$$

for some integer m. This condition is of fundamental importance, and will referred to as "longitudinal phase matching" or just as phase matching. This condition is the spatial analogue of the conservation of energy in time-dependent perturbation theory and therefore may be called as the conservation of momentum.

## 2.3 Coupled-Mode Equations

Equation (23) describes the most general case of mode coupling due to a periodic dielectric perturbation. In practice, often only the coupling between two modes is involved. Let the two-coupled modes be designated as 1 and 2. Neglecting interaction with any of the other modes, the coupled-mode equations become

$$\frac{d}{dz}A_1 = -i\frac{\beta_1}{|\beta_1|}C_{12}^{(m)}A_2 e^{i\Delta\beta z}$$

$$\frac{d}{dz}A_2 = -i\frac{\beta_2}{|\beta_2|}C_{21}^{(-m)}A_1 e^{-i\Delta\beta z} \qquad (26a)$$

where

$$\Delta\beta = \beta_1 - \beta_2 - m\frac{2\pi}{\Lambda} \qquad (26b)$$

And $C_{12}^{(m)}$, $C_{21}^{(-m)}$ are the coupling coefficients given by Eq. (24). It can be shown directly from the definition from Eq. (24) that

$$C_{12}^{(m)} = [C_{21}^{(-m)}]^* \qquad (27)$$

provided that $\Delta\varepsilon$ (x, y, z) is a Hermitian dielectric tensor.

## 2.4 Contradirectional Coupling

When the coupled modes are propagating in opposite directions, say $\beta_1>0$ and $\beta_2<0$, the sign factors $\beta_1/|\beta_1|$ and $\beta_2/|\beta_2|$ become 1 and –1, respectively. The coupled equations become

$$\frac{d}{dz}A_1 = -i\kappa A_2 e^{i\Delta\beta z} \quad ,$$

$$\frac{d}{dz}A_2 = i\kappa^* A_1 e^{-i\Delta\beta z} \quad , \qquad (28)$$

where

$$\kappa = C_{12}^{(m)} \text{ Or } \quad \kappa = \frac{\omega}{4}\int_{-\infty}^{\infty}\varepsilon_1(x)|E_s(x)|^2 dx \qquad (29)$$

The net power in the $+z$ direction for this case is $|A_1|^2$- $|A_2|^2$.The coupled mode equations (28) are again consistent with conservation of energy, which requires that

$$\frac{d}{dz}\{|A_1|^2 - |A_2|^2\} = 0 \qquad (30)$$

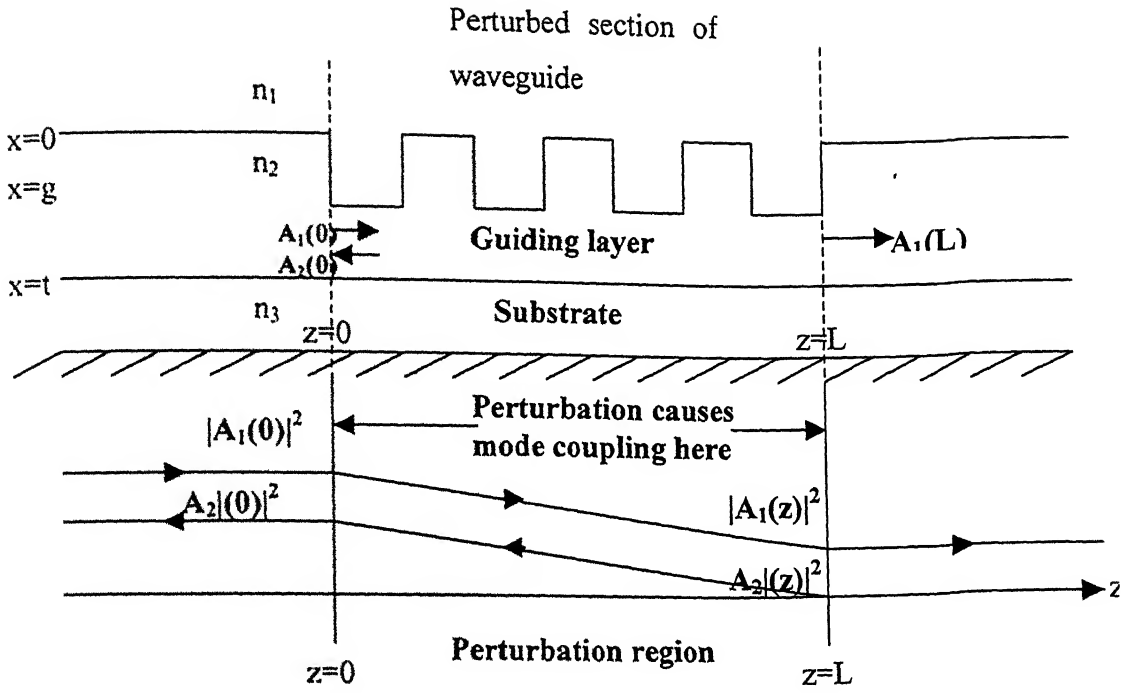


Figure 2.4. Top: a corrugated section of a dielectric waveguide. Bottom: the incident and reflected intensities inside the corrugated section

We now consider the figure shown above, a waveguide with a corrugated section of length L. A wave with an amplitude $A_1(0)$ is incident from left on the corrugated section .In this case, the boundary conditions are $A_1(z)=A_1(0)$ at z=0 and $A_2(z)=0$ at z=L. By substituting $A_1(z)=A_1(0)$ and $A_2(L)=0$ in[11],we obtain the following expressions for the mode amplitudes:

$$A_1(z) = A_1(0)e^{i(\Delta\beta/2)z}\left[\frac{\text{scoshs}(s-L)+i(\Delta\beta/2)\text{sinhs}(L-z)}{\text{scoshsL}+i(\Delta\beta/2)\text{sinhsL}}\right]$$

$$A_2(z) = A_1(0)e^{-i(\Delta\beta/2)z}\left[\frac{-i\kappa^*\text{sinhs}(L-z)}{\text{scoshsL}+i(\Delta\beta/2)\text{sinhsL}}\right] \qquad (31)$$

where s is given by

$$s = \sqrt{\kappa^*\kappa-(\Delta\beta/2)^2} \qquad (32)$$

These expressions are formally identical to those for reflection from a periodic layered medium, except for the coupling constant. The fraction of power coupled to the backward-propagating mode $(-\Delta\beta_s)$, called the mode reflectivity, is defined as

$$R = \left|\frac{A_2(0)}{A_1(0)}\right|^2 \tag{33}$$

and is given according to Eq.(31),by

$$R = \frac{\kappa^* \kappa \sinh^2 sL}{s^2 \cosh^2 sL + (\Delta\beta/2)^2 \sinh^2 sL} \tag{34}$$

## 2.5 Bragg Reflection

Periodic waveguides are guides with a deformation $\Delta\varepsilon$ (x,y,z) that is periodic in z. These guides are used for variety of purposes including the construction of filters, grating couplers, and distributed feedback lasers, and for these purpose of phase matching. The physical process that occurs in such a guide is the scattering of light by the periodic structure, which is similar to the light scattering by a diffraction grating. It can be analysed and viewed as a coupled-mode process.

The optical properties of a periodic medium are described by its dielectric and permeability tensors, which, reflecting the translational symmetry of the medium, are periodic function of z. The simplest periodic medium is one made up of alternating layers of nonmagnetic transparent materials with different refractive indices,where

$$n(z) = \begin{cases} n_2, & 0 < z < d_1 \\ n_1, & d_2 < z < \Lambda \end{cases} \tag{35}$$

with

$$n(z) = n(z + \Lambda) \tag{36}$$

where the z-axis is normal to the layer interfaces and $\Lambda$ is the period. The geometry of

the structure is sketched in Figure.2.4. The coefficient of reflection is given by [11]

$$r_N = \left(\frac{b_0}{a_0}\right)_{b_N=0} \tag{37}$$

that is, the ratio of the complex reflected amplitude $b_0$ at the input to the incident amplitude $a_0$, subject to the boundary condition that to the right of the stack there is no wave incident on it (i.e., $b_N=0$).

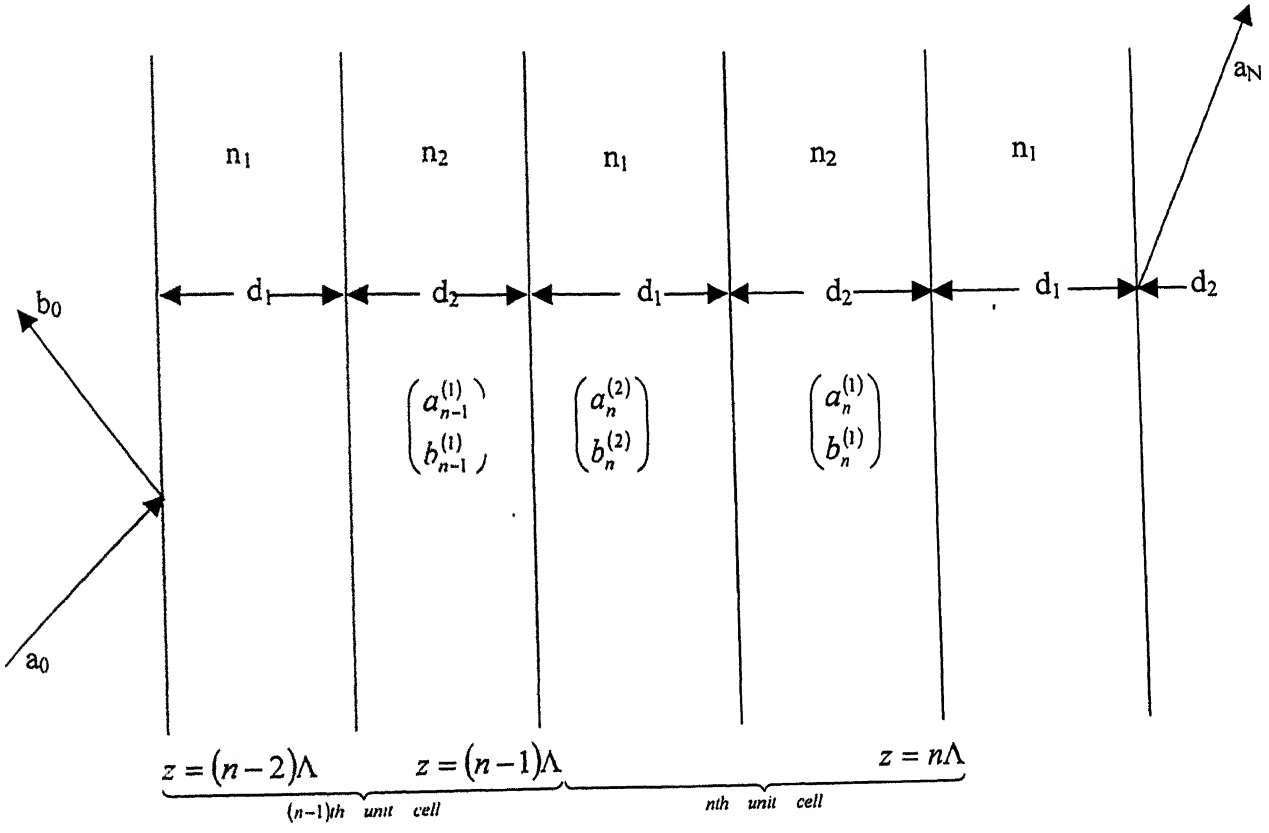


Figure.2.5. A schematic drawing of a periodic layered medium and the plane-wave amplitudes associated with the *n*th unit cell and its neighboring layers

And therefore one may write[11]:

$$\begin{pmatrix} a_0 \\ b_0 \end{pmatrix} = \begin{pmatrix} A & B \\ C & D \end{pmatrix}^N \begin{pmatrix} a_N \\ b_N \end{pmatrix} \tag{38}$$

The Nth power of the unimodular matrix can be simplified by following matrix identity

$$\begin{pmatrix} A & B \\ C & D \end{pmatrix}^N = \begin{pmatrix} AU_{N-1} - U_{N-2} & BU_{N-1} \\ CU_{N-2} & DU_{N-1} - U_{N-2} \end{pmatrix} \tag{39}$$

where

$$U_N = \frac{\sin(N+1)K\Lambda}{\sin K\Lambda} \tag{40}$$

where

$$K(k_y, \omega) = \frac{1}{\Lambda}\cos^{-1}\left[\frac{1}{2}(A+D)\right] \tag{41}$$

with

$$A = e^{ik_{1z}d_1}\left[\cos k_{2z}d_2 + \frac{1}{2}i\left(\frac{k_{2z}}{k_{1z}} + \frac{k_{1z}}{k_{2z}}\right)\sin k_{2z}d_2\right] \tag{42}$$

$$D = e^{-ik_{1z}d_1}\left[\cos k_{2z}d_2 - \frac{1}{2}i\left(\frac{k_{2z}}{k_{1z}} + \frac{k_{1z}}{k_{2z}}\right)\sin k_{2z}d_2\right] \tag{43}$$

The coefficient of reflection is obtained from Eqs. (37), (38), and (39) as

$$r_N = \frac{CU_{N-1}}{AU_{N-1} - U_{N-2}} \tag{44}$$

The reflectivity is obtained by taking the absolute square of $r_N$,

$$|r_N|^2 = \frac{|C|^2}{|C|^2 + \left(\frac{\sin K\Lambda}{\sin NK\Lambda}\right)^2} \tag{45}$$

## 2.6 Analysis of trapezoidal grating

Figure.2.1. shows a schematic view of the corrugated slab waveguide. The functions $\omega_1(x)$ and $\omega_2(x)$ describe the tooth shape, $\Lambda_z$ is the pitch, and g is the tooth height .The waveguide can be composed of several layers, and we assume that the grating is located between layer 1(extending to -∞) and layer 2 (thickness $t_2$). Because of periodicity, the refractive index spatial variation can be written as

$$\Delta n^2(x,z) = \sum \left[A_m(x)\exp\left(2im\pi z/\Lambda\right)\right] \tag{46}$$

with

$$A_m(x) = \frac{n_2^2 - n_1^2}{2im\pi}\left[\exp(-2im\pi\omega_2(x)/\Lambda) - \exp(-2im\pi\omega_1(x)/\Lambda)\right] \tag{47}$$

Using coupled mode theory, the coupling coefficient κ is expressed as [5]

$$\kappa = \frac{k_o^2}{2\beta N^2}\left|\int_{corrugation} A_m(x)E^2(x)dx\right| \tag{48}$$

where $k_o = 2\pi/\lambda_o$ is the free-space propagation constant, β is the mode propagation constant, E(x) is the y component of the unperturbed electric field, and $N^2$ is a normalisation constant given by

$$N^2 = \int_{-\infty}^{\infty} E^2(x)dx \tag{49}$$

In [6] the full guide width $t$ (see Fig. 2.1) was employed to compute the unperturbed mode field E. The optimal unperturbed mode E is that of a related four-layer structure (see [6]); however, we have found that one can obtain adequate accuracy without excessive complexity by judiciously choosing the unperturbed guide boundary at $t' < t$. We choose t' such that the volume of $n_1$ material extending into region 2 just equals the volume of $n_2$ material extending into region 1. The symbol t' thus refers to the distance from $n_2$-$n_3$ interface to the line .The unperturbed mode E(x) is then

$$E(x) = \begin{cases} \exp(qx), & x \le 0 \\ \cos(hx) + (q/h)\sin(hx), & 0 \le x \le t' \\ [\cos(ht') + (q/h)\sin(ht')]\exp[-p(x-t')], & t' \le x \end{cases} \tag{50}$$

where

$$\begin{aligned} q &= \sqrt{(\beta^2 - n_1^2k_0^2)} \\ h &= \sqrt{(n_2^2k_0^2 - \beta^2)} \\ p &= \sqrt{(\beta^2 - n_3^2k_0^2)} \end{aligned} \tag{51}$$

and where β is found by solving

$$\tan(ht') = \frac{h(q+p)}{h^2 - pq} \tag{52}$$

and

$$N^2 = \int_{-\infty}^{\infty} E^2(x)dx = \frac{\left(h^2+q^2\right)\left(t'+q^{-1}+p^{-1}\right)}{2h^2} \tag{53}$$

For trapezoidal grating under consideration.

$$\begin{aligned} \omega_1(x) &= x\tan\theta t + d_1 + d_2 - g\tan\theta \\ \omega_2(x) &= x\tan\theta + d_2 - g\tan\theta \end{aligned} \tag{54}$$

$$\omega_1(x) = \Lambda - \omega_2(x) = \frac{L_1}{2} + L_2\frac{x}{g} \tag{55a}$$

$$\bar{g} = g\left(1 - \frac{L_1+L_2}{\Lambda}\right) \tag{55b}$$

$$\bar{\omega} = \omega_1(\bar{g}) = \frac{L_1}{2} + L_2\frac{\bar{g}}{g} \tag{55c}$$

$$\omega = \omega_1(g) = \frac{L_1}{2} + L_2 \tag{55d}$$

$$A_m(x) = \frac{n_2^2 - n_1^2}{m\pi}\sin\left[\frac{2m\pi}{\Lambda}\left(\frac{L_1}{2} + L_2\frac{x}{g}\right)\right] \tag{55e}$$

with the assumption that the waveguide geometry is such that the unperturbed electric field is exponentially decreasing in layer 1, sinusoidal in layer 2, exponential in layer 3, taking into account the boundary conditions concerning E and dE/dx at $x=\bar{g}$, we deduce that E can be written as

$$\begin{aligned} &x \le \bar{g}, \quad E(x) = e^{P_1(x-\bar{g})} \\ &\bar{g} \le x \le t_2, \qquad E(x) = \cos[K_2(x-\bar{g})] + \frac{P_1}{K_2}\sin[K_2(x-\bar{g})] \end{aligned} \tag{56}$$

where $P_1$ and $K_2$ are the transverse propagation constants in layers 1 and 2.

# Chapter 3

# RESULTS AND DISCUSSIONS

This chapter presents the results of this work. In the first part, the computed values of the reflection coefficient of the Bragg Gratings with varying wavelength and distance are given. In the second part, reflection coefficients of the misaligned grating are computed at various parameters.

## 3.1 Reflection Coefficient of Bragg Gratings.

The reflection coefficient is computed from the Eq.(38) . Fig.3.1 to Fig.3.4 gives the computed reflection coefficients as a function of distance $d_1$ where the period of the grating is $d_1+d_2$ and $d_2$ is given by $(n_2/n_1)d_1$ and as a function of wavelength.

At lower values of the number of periods the reflectivity is very low of the order of 0.1% for N=10 but as the number of periods increases the reflectivity goes up.

It is clear from the figures that as we increase the number of periods in grating the reflection coefficient increases. As the wavelength is increases the reflectivity curve shifts towards right. It is also clear from the above graph that the wavelength spectrum repeats after a wavelength and it's reflection coefficient is also a function of grating period.

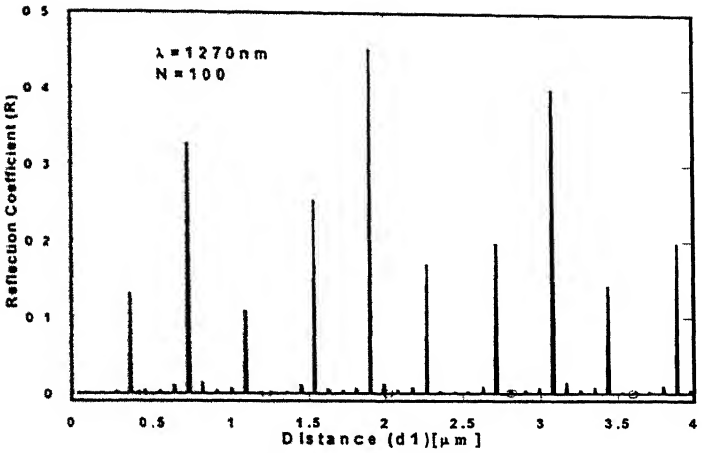


(a)

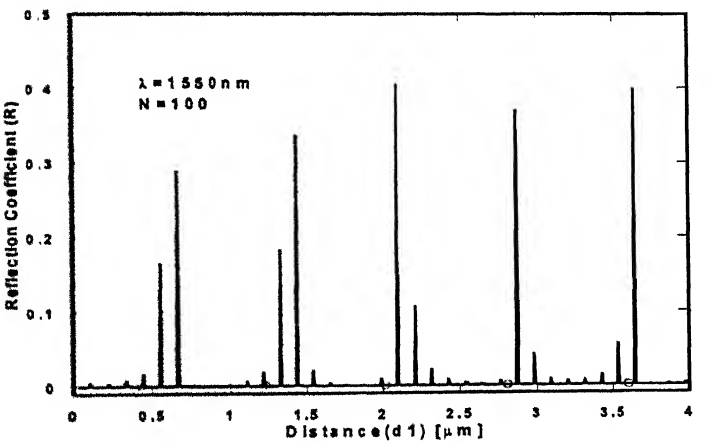


(b)

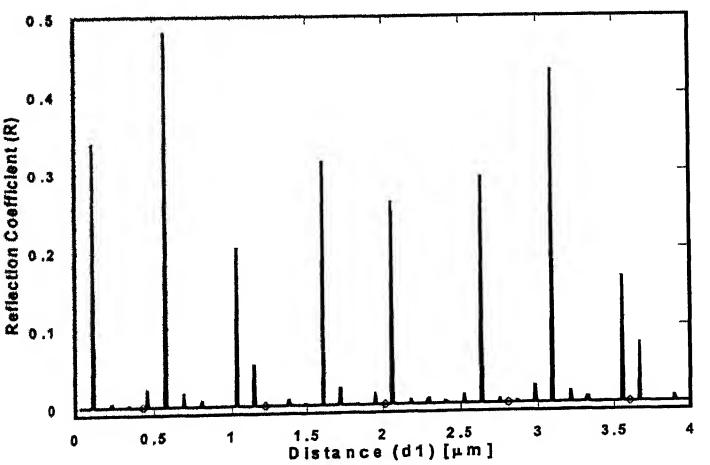


(c)

Figure.3.1. Distance ($d_1$) dependence on Reflection Coefficients at various Wavelength with N=100

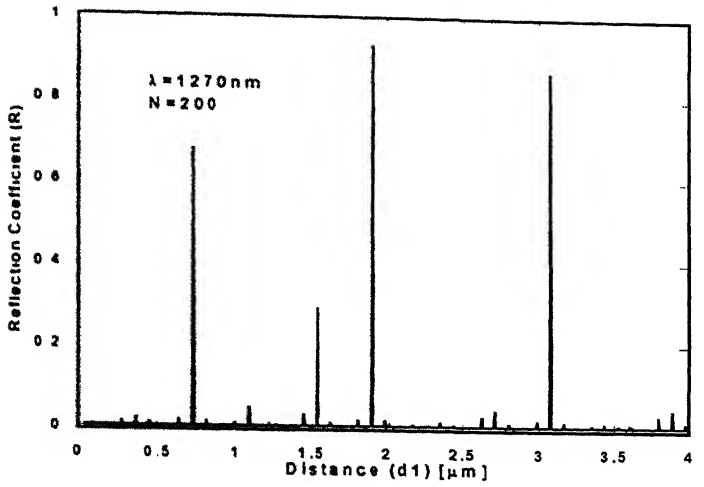


(a)

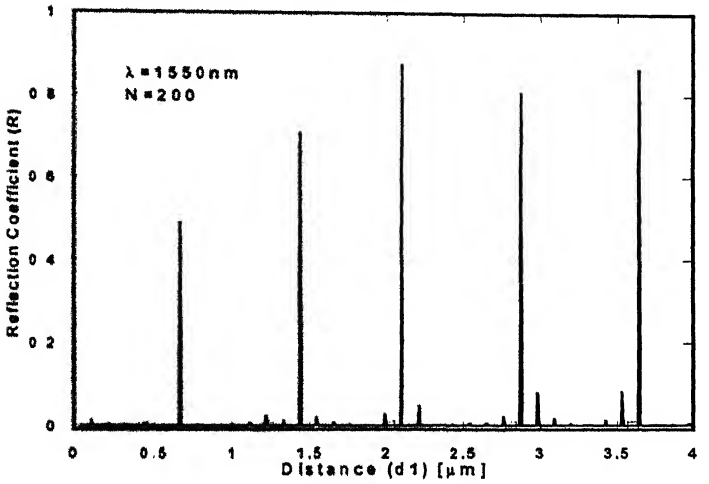


(b)

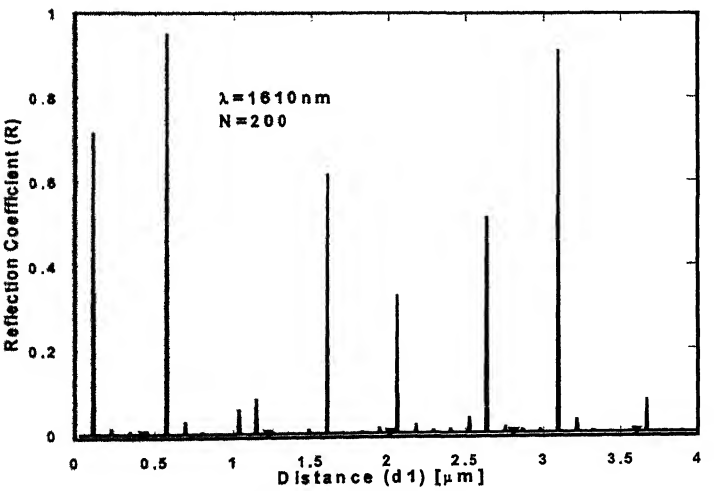


(c)

Figure.3.2. Distance ($d_1$) dependence on Reflection Coefficients at various Wavelength

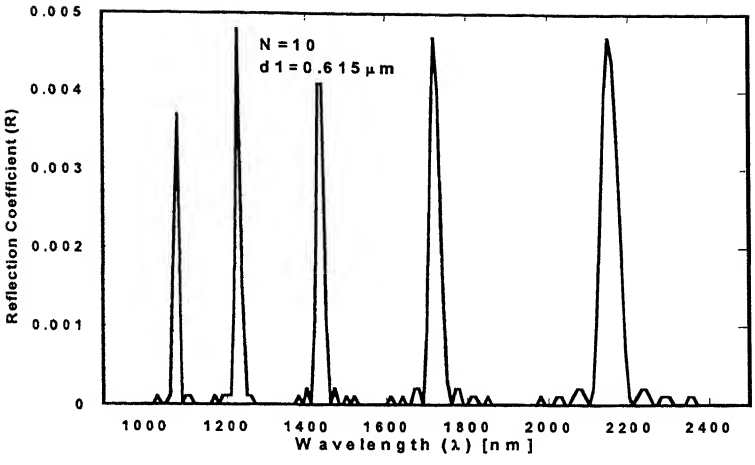


(a)

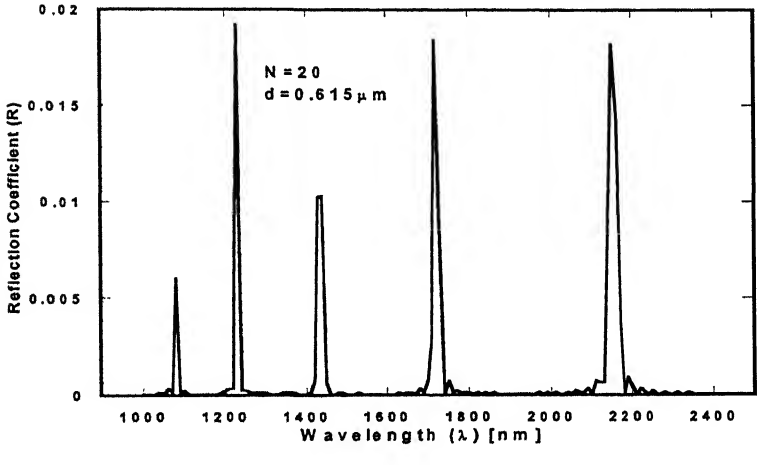


(b)

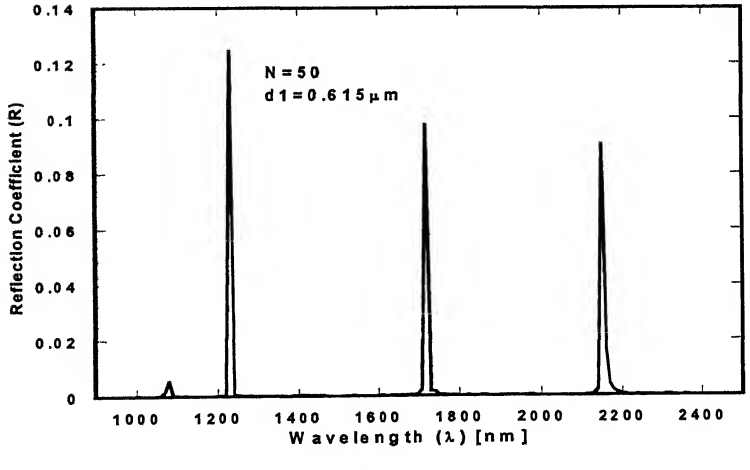


(c)

Figure.3.3. Wavelength (λ) dependence on Reflection Coefficients at various N with Distance ($d_1$=0.615μm)

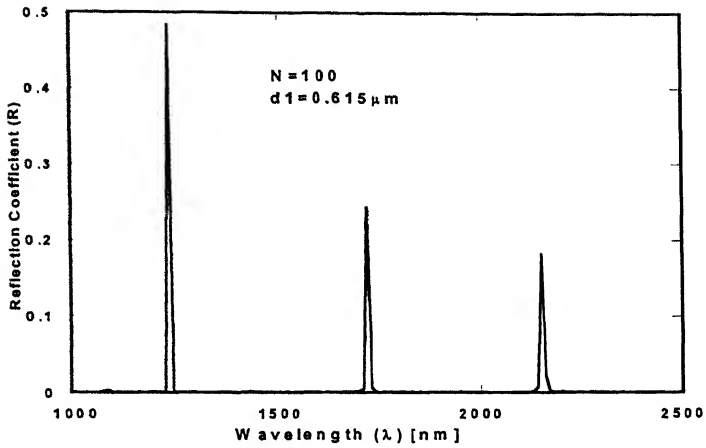


(a)

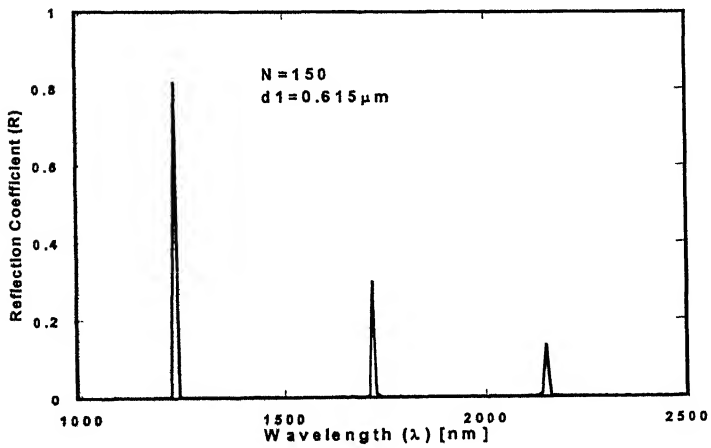


(b)

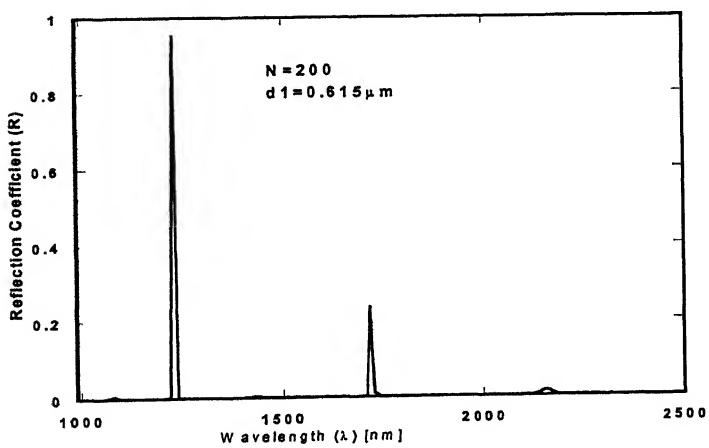


(c)

Figure.3.4. Wavelength (λ) dependence on Reflection Coefficients at various N with

## 3.2 Reflectivity of the Trapezoidal grating.

The reflection coefficient and coupling coefficients of the trapezoidal grating is computed using Eqs. (34) and (48) respectively.

### 3.2.1. Reflectivity Vs Distance.

From the above graphs it is clear that as we increase the wavelength we get the value of d in between 0.4 micrometer to 0.6 micrometer, which is the prime requirement for the fabrication of the grating and the reflectivity shift towards right as the wavelength increases so we can get the response of the grating in the range of 1270nm to 1610 nm which is the required range for the CWDM with dopant window of the order of 0.5 to 0.6 micrometer.

From the above plots the possibility of adjusting $L_2$ to the expected value of $d_1$ is a considerable advantage offered by the ion beam etching technique, and should therefore lead to high coupling coefficients and reflection coefficient.

In Figure 3.9.comparison of the second mode reflection coefficients of the grating at wavelength Separations of 20nm as required for Coarse Wavelength Division Multiplexing. The plot shows that for practical cases we need 80nm separation for less cross talk.

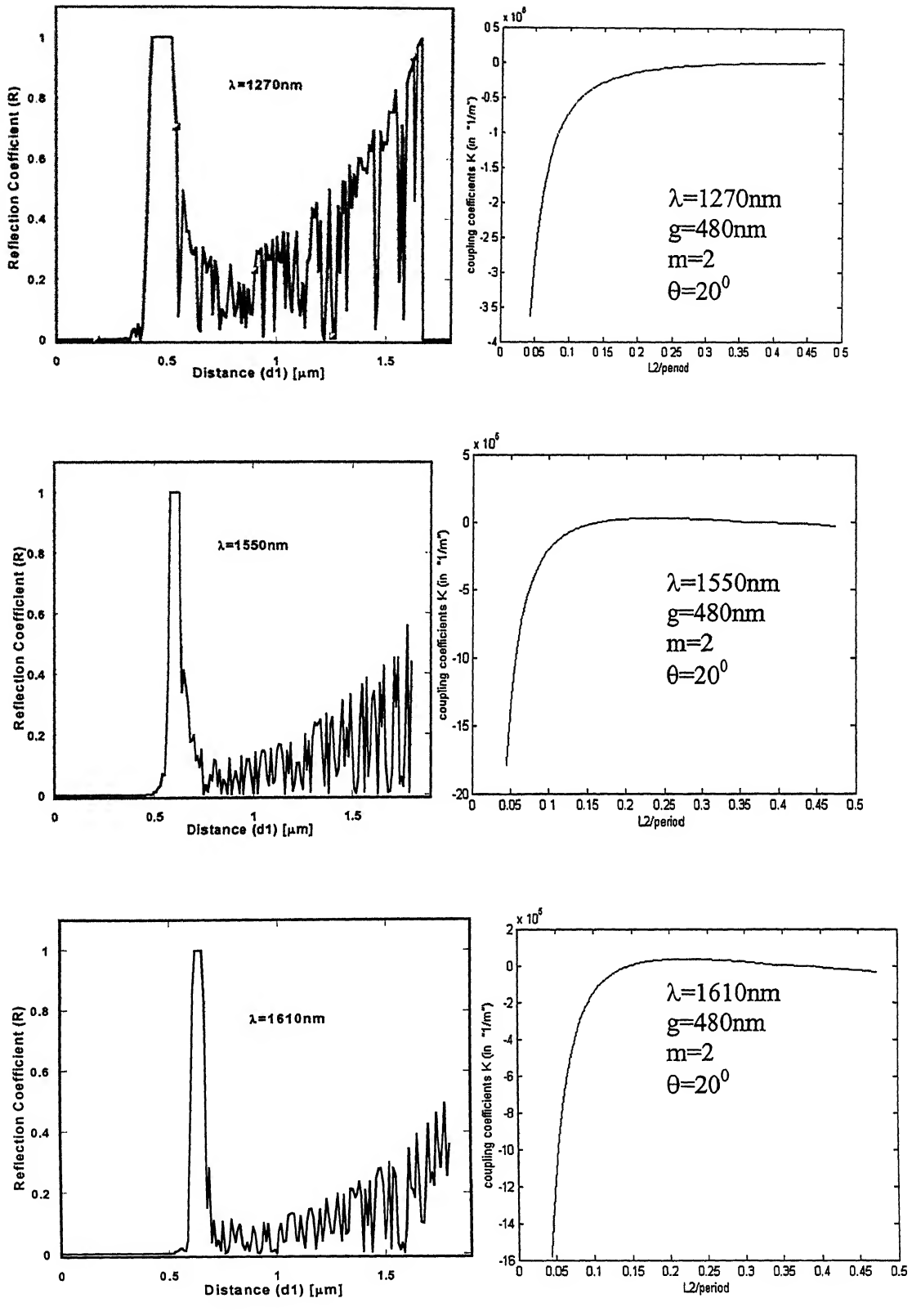


(a) (b)

Figure.3.5. (a) Reflection Coefficient as a function of Distance $d_1$ at various wavelength with groove height 'g' of 480 nm, m=2 and angle is 20°.
(b) Coupling Coefficient as a function of Normalised Distance ($L_2/\Lambda_z$ )at various wavelength with groove height 'g' of 480 nm, m=2 and angle is 20°.

## 3.2.2 Reflectivity Vs Groove Height.

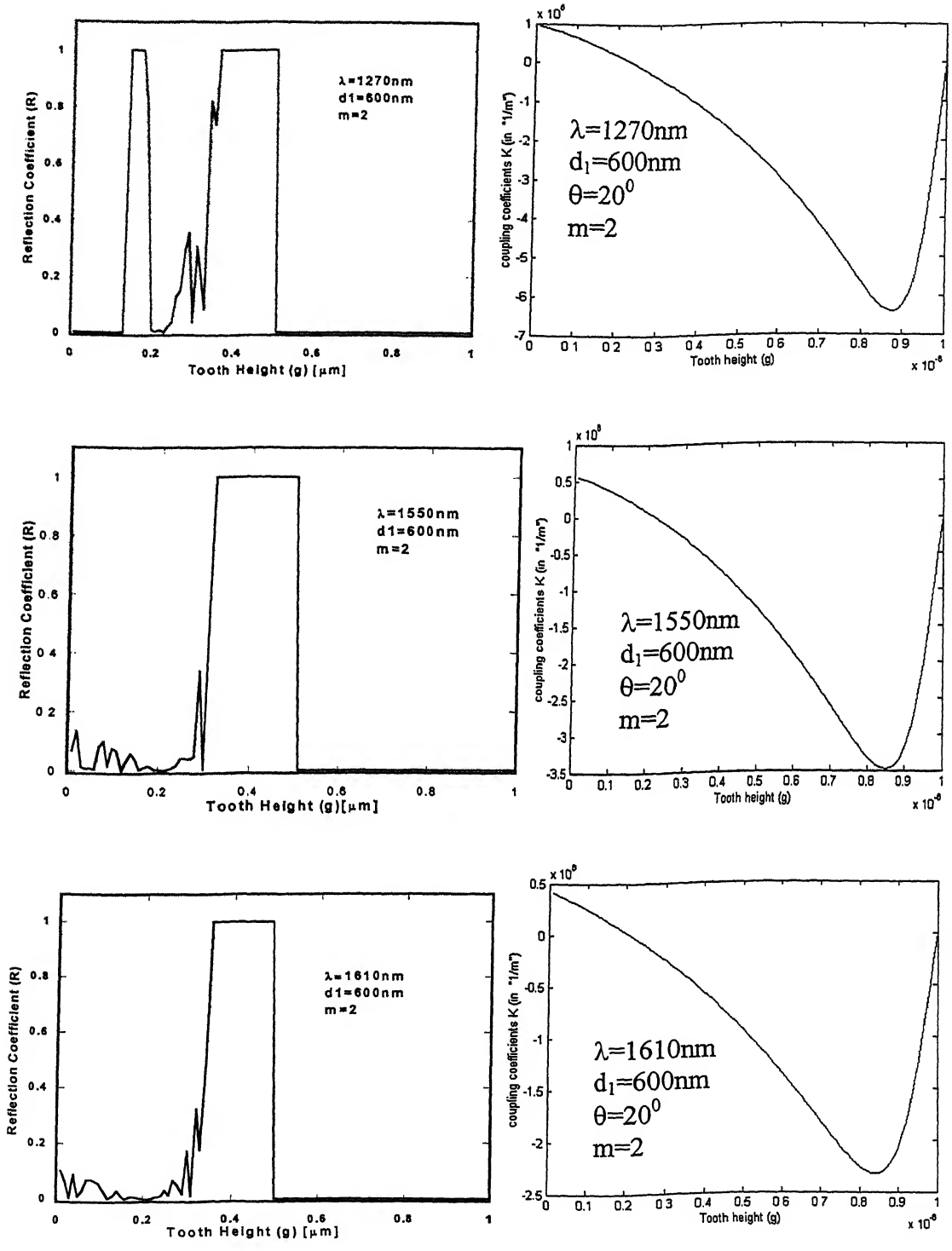


(a) (b)

Figure.3.6.(a) Reflection Coefficient as a function of Tooth Height (g) [μm]at various wavelength with Distance '$d_1$' of 600nm, m=2 and angle is 20°

(b) Coupling Coefficient as a function of Tooth Height (g) [μm] at various wavelength with Distance '$d_1$' of 600nm, m=2 and angle is 20°.

The reflectivity is calculated as varying groove height with wavelength as the parameter from the given graph it is clear that the grating response is good for the groove height of the order of 0.4 micrometer to 0.5 micrometer as we increase the wavelength keeping the angle of tilt 20 degree .As we increase the angle we get the range of groove height decreases as well as the reflectivity is not good.

### 3.2.3 Reflectivity Vs Mode Number.

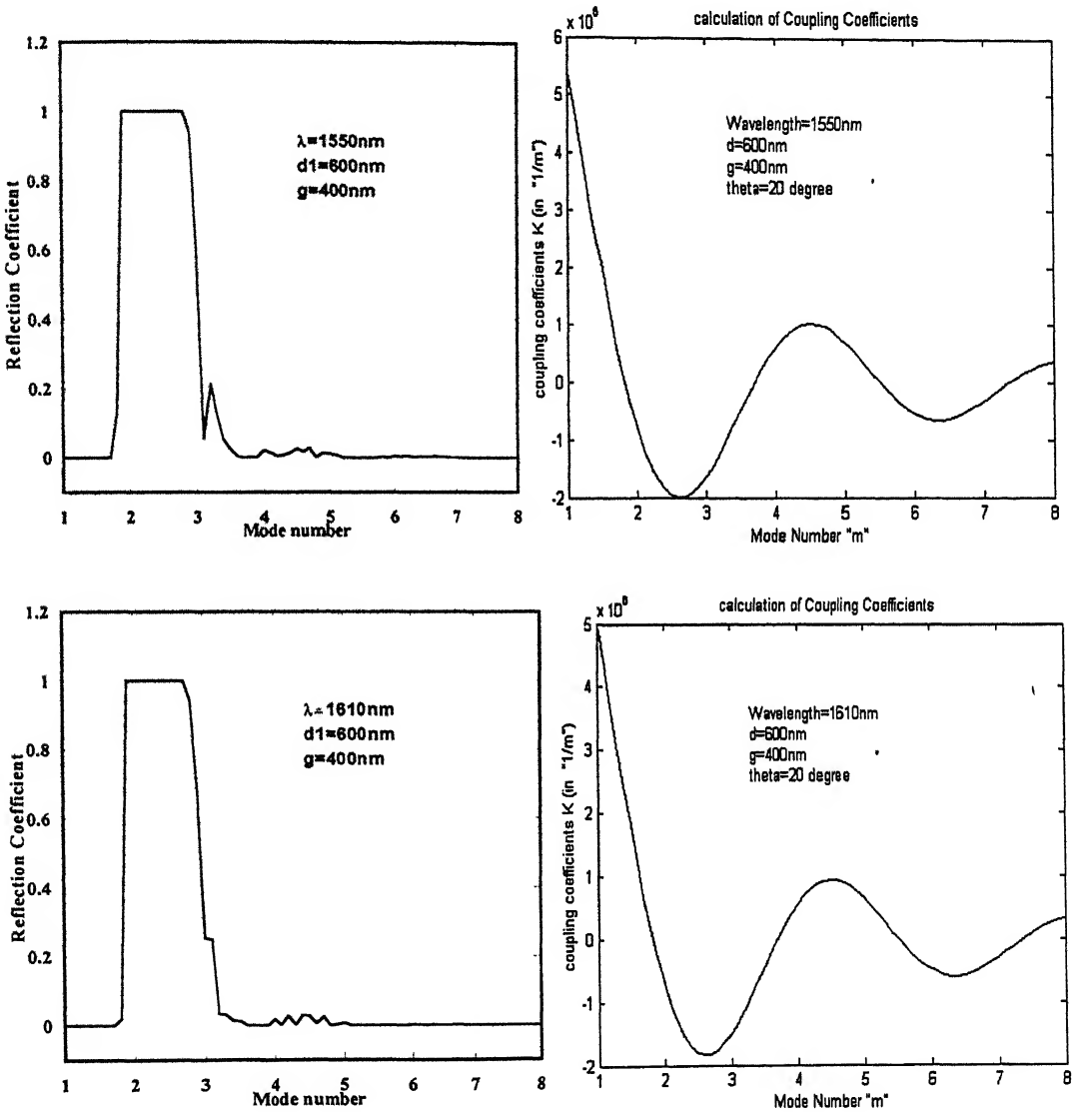


(a) (b)

Figure.3.7.(a) Reflection Coefficient as a function of Mode Number at various wavelength with distance of 600 nm, groove height of 400nm and angle is $20^0$

(b) Coupling Coefficient as a function Mode Number at various wavelength with distance of 600 nm and angle is 20 degree

From the above graphs it is clear that for m=2 the reflectivity response is coming good. From the given graph it is clear that we have optimum value of coupling coefficient in the second order mode.

### 3.2.4 Reflectivity Vs Wavelength.

Using the above computed values of distance, groove height and mode number we calculated the reflectivity with wavelength. From the graphs given below we find that the response of the grating is very good in the range of 1270nm to 1610 nm. As we increase the wavelength in the interval of 20nm it shift towards the right.

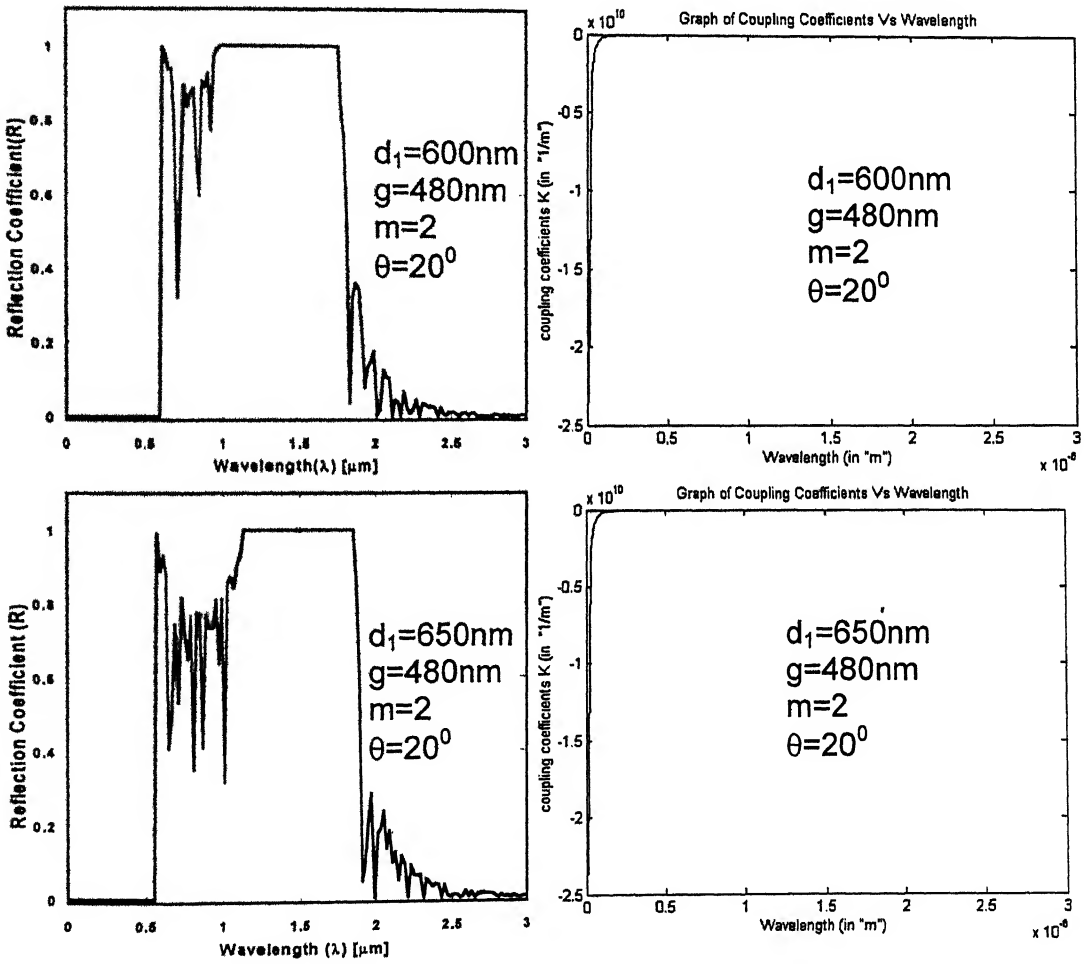


(a) (b)

Figure.3.8. (a) Variation of Reflection Coefficient with Wavelength at various Distance $d_1$ [nm] with groove height of 480nm, angle is $20^0$ and m=2.

(b) Variation of Coupling Coefficient with Wavelength at various Distance $d_1$ [nm] with groove height of 480nm, angle is $20^0$ and m=2.

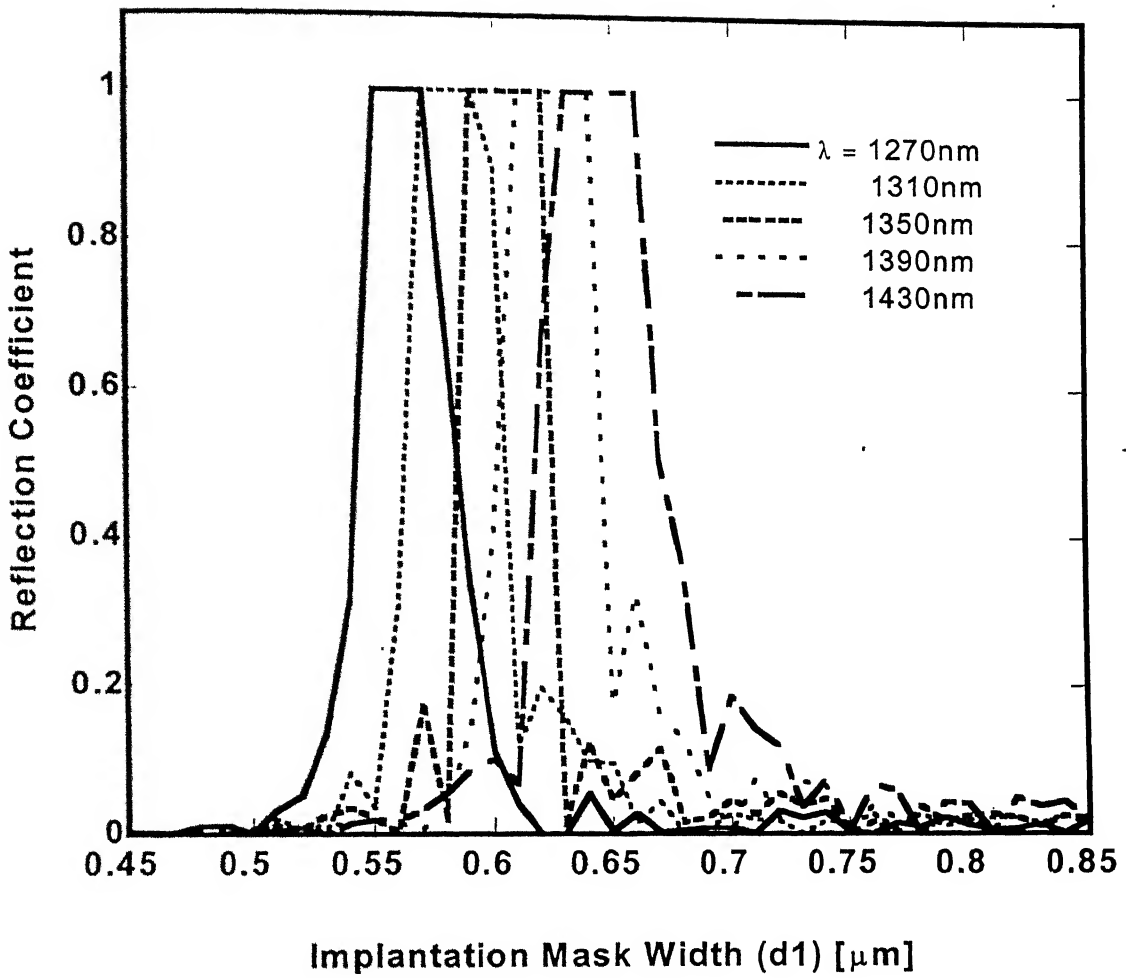


Figure 3.9.Comparison of the second mode reflection coefficients of the grating at wavelength Separations of 20nm as required for Coarse Wavelength Division Multiplexing at

# Chapter 4

# CONCLUSIONS

I have been applied in this work of coupled modes to describe a wide range of experimental situation in guided-wave optics. The computed value of reflection coefficients for Bragg's grating, coupling coefficient and reflection coefficient for TE modes in the preceding of trapezoidal corrugation shape is based on perturbation analysis. The analysis has been done for both first order and second order gratings. First order grating show larger discrimination however their physical dimensions are difficult to realize by simple photolithography. Second order grating show that they are realizable for 1270nm-1610nm-wavelength range for periodic dimensions of 0.5-1.2μm. Practical cases of periodic change in the refractive index by Impurity Implantation Disordering of quantum wells have also been considered.

The simulation results shows (1) as increase in the wavelength results right shift in the groove depth. (2) Similarly increasing the wavelength results right shift in the distance ($d_1$). In practical case 40nm separation between the wavelengths will results more cross talk as compared to 80nm separation. (3) From the plot reflectivity with mode number shows the mode number 2 is the best choice for practical implementation and (4) from the graph of reflectivity with wavelength shows that a very good response for the trapezoidal grating only in the wavelength region of 1.27μm-1.61μm.

The results indicate optimum parameter values to maximize reflection coefficient. In particular results shows that their exit optimal tooth heights and that the

grating period should be as large as possible to maximize reflection coefficients and coupling coefficient. The analysis yields parametric dependences that should prove useful in the understanding of grating-coupled surface emitters. The results indicate that it is often desirable to fabricate the DFB grating of a guided wave laser at a period which differs substantially from that required to resonate the lowest order mode.

# REFERENCES


[1] D.R.Scifres, R.D.Burnham, and W.Streifer, "Distributed-feedback single heterojunction GaAs diode laser,"*Appl.Phys.Lett.*, vol.25, pp.203-206, 1974.

[2] S.Wang, "Principles of distributed-feedback and distributed Bragg-reflector lasers,"*IEEE J.Quantum Electron.*, vol. QE-10, pp.413-427, Apr.1974.

[3] D.C.Flanders, H.Koegelnik, R.N.Schmidt, and C.V.Shank, "Grating filters for thin-film optical waveguides," *Appl.Phys.Lett.*, vol.24, pp.194--196, 1974.

[4] A.C.Livanos, A.Katzir, A.Yariv, and C.S.Hong, "Chirped-grating demultiplexers in dielectric waveguides," *Appl.Phys.Lett.*, vol.30, pp.519-521, 1977.

[5] W.Streifer, D.R.Scifres, and R.D.Burnham. "Coupling coefficients for distributed feedback single-and double-heterostructure lasers," *IEEE J.Quantum Electron.*, vol. QE-11, pp.867-873, 1975.

[6] A.Yariv, "Coupled-mode theory for guided wave optics," *IEEE J.Quantum Electron.*, vol. QE-9, pp.919-933, Sept.1973.

[7] H.Kogelnik and C.V.Shank, "Coupled-wave theory of distributed feedback lasers," *J.Appl.Phys.*, vol.43, pp.2327-2335, 1972.

[8] A.Hardy, "Exact derivation of the coupling coefficient in corrugated waveguides with rectangular tooth shape,"*IEEE J.Quantum Electron.*, vol. QE-20, pp.1132-1138, 1984.

[9] Tamir, T. "*Integrated Optics*", Springer-Verlarg, New York, 1975.

[10] W. Streifer, D.R.Scifres, and R.D.Burnham, "Periodic corrugated dielectric waveguides, "*Fiber Integrated Opt.*, vol. 1,1985.

[11] A.Yariv and P.Yeh, ."*Optical Waves in Crystals*", John Wiley & Sons publication 1984.